OMAE2013-10473

EXPERIMENTAL INVESTIGATION OF VIM CHARACTERISTICS ON COLUMN TYPE FLOATER IN SUPER CRITICAL REYNOLDS NUMBER

Toshifumi Fujiwara
Ocean Engineering Department

Masakatsu Saito
Ocean Engineering Department

Katsuya Maeda
Ocean Engineering Department

Hiroshi Sato
Ocean Engineering Department

Kei Ishida
Ocean Engineering Department

National Maritime Research Institute
Tokyo, Japan

ABSTRACT

In Japan, floating wind turbine facilities are planned to be set in the offshore, where bottom-mounted type's one is not feasible, to generate natural resource electricity. One of the ways for application is that the facilities are mounted on a column type floater to keep buoyancy and stability in the sea that is called as Spar type. At that time, the characteristic of VIM, i.e. Vortex Induced Motion, on the column type floater is concerned about to maintain mooring safety of the wind turbine.

VIM characteristic on the column type floater was investigated using a huge experimental model in supper critical Reynolds number at the large towing tank in the National Maritime Research Institute, Japan.

The results of the experiment were compared with ones of a small similar figure model under critical Reynolds number, and VIM amplitudes against reduced velocity parameter are clearly understood. The amplitude distribution relating to duration time for large VIM amplitude is also investigated to assess the effect on fatigue damage of mooring lines. These unique and precious results have important role for making the safety guideline on mooring requirement on a column type floater.

INTRODUCTION

Natural energy resources that is no or minimum stress for global environment are demanded for developing comfortable life of humanity. In those, wind force energy is attracted in worldwide because of ease acquisition. In Japan, there are land characteristics that mountains are steep in the narrow land area band and seashores become deep rapidly. The excelled constant wind energy resource is in offing area where is rather far from land and bottom-mounted types are not feasible. Then, floating wind turbine facilities are planned in our country to be set in the offshore as floating type.

Figure 1. Spar type floating wind turbine image.

A Spar type floater like shown in Figure 1 is selected as the base unit of a wind turbine from viewpoint of easy construction and maintenance, but the problem of VIM that may cause damage to mooring lines, cannot be bypassed. In ocean engineering researches, VIM is popular topic and many researchers have been concerned in many years. For instance, tank test results of a Spar type floater are compared with the field measurement data with a full scale Spar [1][2]. As a result, these outcomes have been reflected in ISO and API standard documents [3][4]. Recently Finnigan et al. had conducted the Spar model experiments in the basin in super critical Reynolds

number [5]~[7]. It is hard, however, to say that the VIM phenomenon was enough solved since VIM phenomenon is strongly dependent on form of an object structure, and in the full scale measurement, various error factors are included from change of ocean condition. Computational researches seem also not to catch up with representing the phenomenon in the simulation and estimating VIM [8].

As a rare trial, VIM characteristics on the basic column type floater were investigated using the huge test model (Length (Depth)×Diameter=5.0×1.5m, about 1/10 for the real floater) in supper critical Reynolds number at the 400m towing tank in the National Maritime Research Institute, Japan. The results of the experiment were compared with the small similar figure model (L×D=1.0×0.3m, about 1/50 for the real floater), that may be ordinary used in the model test for reason of easy treatment, under critical Reynolds number. Maximum VIM amplitudes against the reduced velocity parameter are clearly understood from the two different size models' experiments. The amplitude distribution for VIM is also investigated to assess the effect on fatigue damage of mooring lines and decide on the safety level of VIM amplitude in the domestic safety guideline.

KEYWORDS
Vortex Induced Motion (VIM), Spar, Column, Super Critical Reynolds Number, Model Experiment.

EXPERIMENT
Model
Large and small simplified Spar models were prepared for experiments. Table 1 shows the model specifications and Figure 2 and 3 show appearance of the models. The large Spar model, here called as 'L-model', has simple column form, 1.5m diameter, 5m length and about 8ton displacement. On the other hand, a small model called as 'S-model' has analogue form of the L-model, 0.3m diameter, 1m length and 64kg displacement. The L-model was made of iron and the S-model of acrylic resin, which the surface of the L-model was only coated with paint and nothing is done for the S-model.

Experimental condition
Table 1 also represents the experimental conditions. The reduced velocity V_r and the Reynolds number R_e following definitions are about 3.9~18 and 1.5~7.0×10^5 in case of the L-model respectively.

$$V_r = V/(f_n D) \tag{1}$$
$$R_e = VD/\nu \tag{2}$$

where V ; Current velocity that is towing velocity in the experiment, f_n (=1/T); Natural frequency of transverse motion decided by mooring lines characteristics, T ; Natural period, D ; Diameter of model, ν ; Coefficient of kinematic viscosity.

The natural frequency of transverse motion, f_n is defined as follows:

$$f_n = \frac{1}{2\pi}\sqrt{\frac{k}{M}} \tag{3}$$

where k ; Transverse stiffness, M ; Total mass in towing.

Table 1. Experimental models.

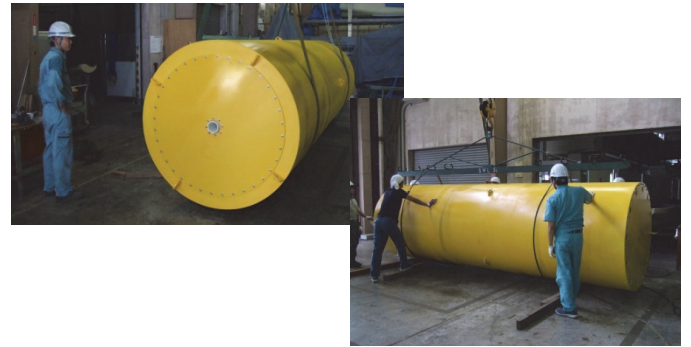| Item	Unit	Large Spar (L-model)	Small Spar (S-model)
Diameter (D)	m	1.5	0.3
Length (L)	m	5.0	1.0
Draft (d)	m	4.5	0.9
Displacement (W)	kg	7952	64
Sway natural period (T)	s	30, 58	15
Towing velocity (V)	m/s	0.10〜0.45	0.08〜0.23
Reduced velocity (Vr=VT/D)	-	3.9〜17.7	3.4〜9.7
Reynolds number (Re=VD/v)	-	1.5〜7.0×10^5	2.4〜6.9×10^4

Figure 2. Large Spar model (L-model).

Figure 3. Small Spar model (S-model).

Experimental facilities and setting
Experiments were carried out in our research institute. For the L-model, the 400m towing tank (L400×B18×D8m) shown in Figure 4 was used because of long towing distance and deep tank size. It is possible to do this experiment like in the extremely steady current condition using the towing carriage

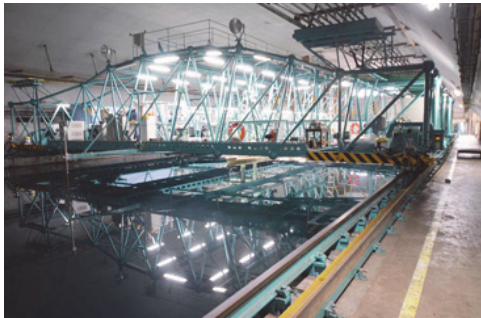Figure 5 shows experimental situation at the 400m towing tank used for the L-model.

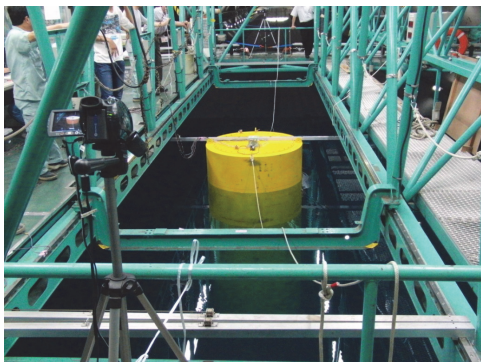**Figure 4.** 400m towing tank used for the L-model.

Figure 5. Experimental situation at 400m towing tank used for the L-model.

Figure 6. Actual sea model basin used for the S-model.

For the S-model, the Actual sea model basin was utilized for the experiment. The size of the basin is L80×B40×D4.5m, and 382 wave makers are equipped in all around of the basin, that is unique seakeeping test facility as shown in Figure 6. Experimental situation at the basin using the S-model is shown in Figure 7.

Figure 8 describes experimental mooring and position sensing conditions of the L-model, that is same situation in case of the S-model. Figure 9 shows top view on experimental mooring condition of the L- and S-models. Spring stiffness decides natural frequency of the model motion. As shown in Table 1, the natual period, T is set to 30s, 58s for the L-

model and 15s for the S-model. A CCD camera at the top of the carriage with LED makers on the model were used to catch the model position. A optical fiber gyroscope was set to measure pitch and roll motion of the L-model, but in the experiment those motions to be especially mentioned in here were not observed.
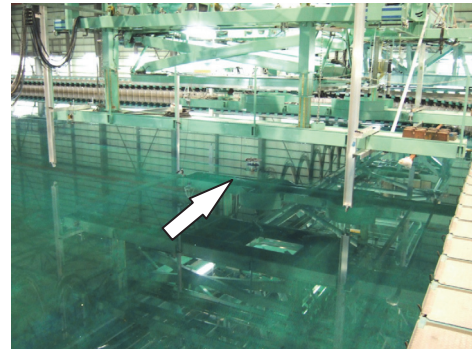

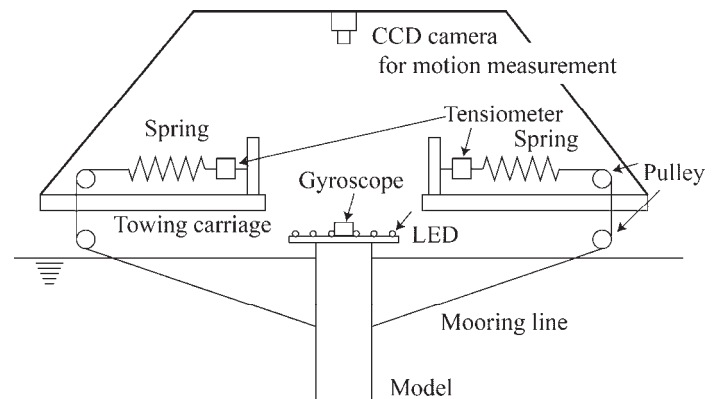**Figure 7.** Experimental situation at Actual sea model basin used for the S-model.

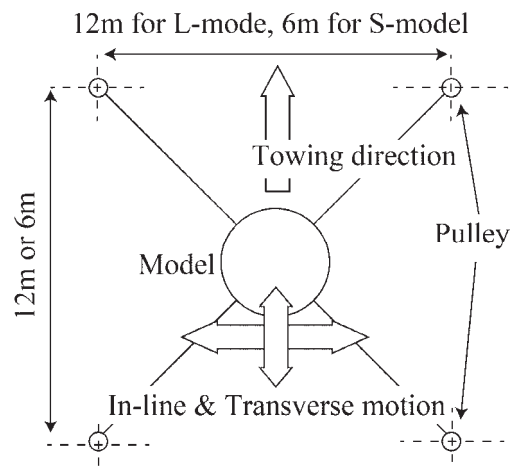**Figure 8.** Experimental mooring condition and position sensing of the L-model.

Figure 9. Top view on experimental mooring condition of the models.
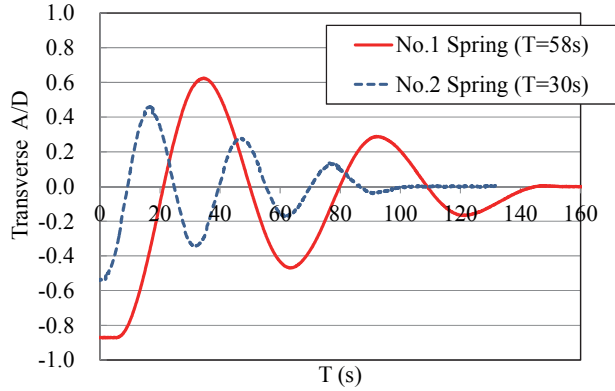
3

Figure 10. Example of free damping tests of the L-model using 2 kinds of springs.

As a reference, the result of free damping tests of the L-model using 2 kinds of springs is shown in Figure 10. The damping ratio of the L-model is obtained as 12% critical damping after averaging No.1 and No.2 cases.

EXPERIMENTAL RESULTS

At first, the result of drag coefficient is shown in Figure 11. The drag coefficient presented in this paper is defined as follows:

$$C_D = \frac{F_X}{1/2 \, \rho D d V^2} \qquad (4)$$

where F_X; In-line direction force, ρ; Density of water, d; Draft.
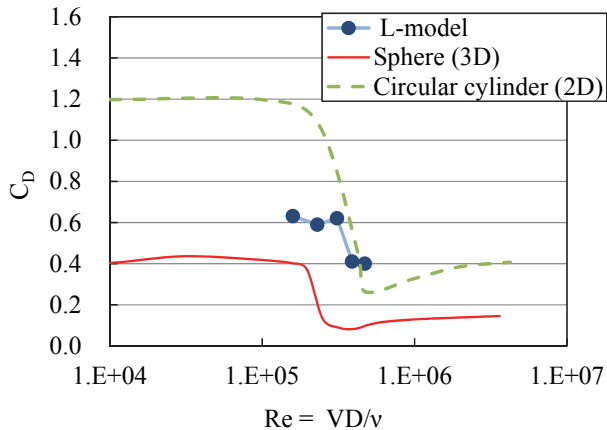

Figure 11. Drag coefficient of the L-model comparing with those of spheres and circular cylinders.

The drag coefficient of the L-model is comparing with that of spheres and 2-dimensional circular cylinders consisted of many data resources [9]. This L-model drag data were obtained in towing not developping VIM phenomenon. In the experimental data, there are two stages, one is the previous

situation of critical Reynolds number, $R_e < 4 \times 10^5$ (V =0.1~0.2m/s), and the other is in the high Reynolds number going over critical region, $R_e \geq 4 \times 10^5$ (V =0.25~0.3m/s). In this paper, the former condition that is relatively smaller Reynolds number corresponded to under critical is named as 'UC-Re', and the latter condition that is equal to super critical Reynolds region is named as 'SC-Re'. The L-model's hydrodynamics characteristic in the Figure 11 seems to be placed as the middle quality in the 2-D cylinder and 3-D sphere, then authors judge $R_e \geq 4 \times 10^5$, defined as SC-Re, is in the super critical Reynolds region for this L-model. The aim of this time experiment is to understand clearly the phnomenon of the super critical Reynolds number region considered as same situation of VIM phenomenon for a real Spar.
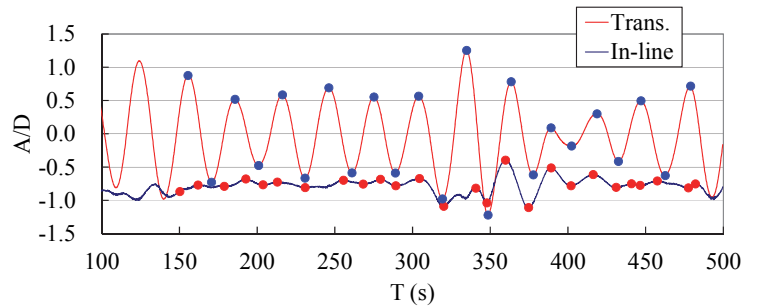

Figure 12. Example of time series on amplitude in each direction of the L-model in V_r =9.2.

Example of time series on amplitude in transverse and in-line directions of the L-model in V_r =9.2 is represented as Figure 12. The transeverse amplitude is largely changed as shown in the figure. Peak values marked with bule dots for transverse and red dots for in-line motion are picked up for following analysis.

Figures 13 and 14 show the mean and maximum amplitude of transverse motion in two different Reynolds number region. The holizontal axis is V_r defined in Eq.1. The mean and maximum values divided by the model diameter D are plotted in the figures. Here, the 'mean' is averaged value of peak values marked with bule dots in the Figure 12 in one trial towing about 300m and the 'max' is defined as the mean value added 2 times standard deviation σ of the amplitude.

Experimental results of the L-model and S-model in the UC-Re are generally coincided each other. On the other hands, SC-Re's results are lower than them, that the maximum value of A_{max}/D in the Figure 14 is about 1.0, and that of A_{mean}/D is about 0.6~0.7 from Figure 13. In the same figure, the indicated values in the reference [10, OTC15245] are drawn as dotted lines, which are referred in the API Recommended Practice 2SK [4]. When assuming the dotted line of 'Sensitivity case2' is mean value of VIM amplitude, maximum value level of A_{mean}/D of the L-model experimental results in SC-Re is same level for reference lines.
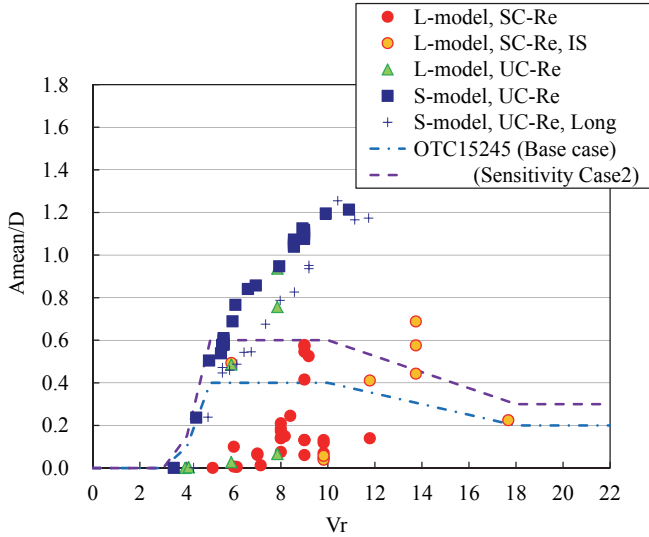
Figure 13. Mean amplitude of transverse motion of the models in two different Reynolds number region.
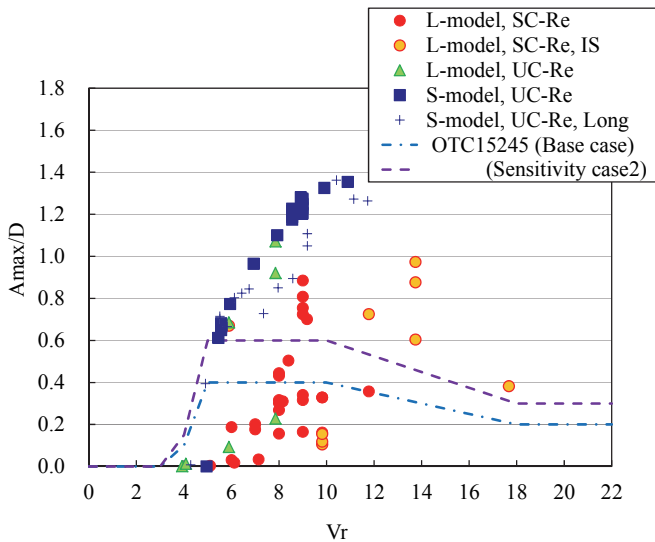

Figure 14. Maximum amplitude of transverse motion of the models in two different Reynolds number region.

Basically each test was conducted in no initial transverse shift, that means transverse oscillation naturally and gradually progresses or not. On the other hand, 'IS' in the figures means initial shift was artificially added in each test as progressing transverse motion rapidly. Excepting initial time series enoughly to remove the initial shift effect, analysis of the IS test series was done. As a result, since the transverse amplitude by the initial shift vanishes soon at the beginning stage, the IS trial doesn't have intended mean.

For a strength design criteria, the result of A_{max}/D shown in Figure 14 may become important. As it is not comfortable to use the indicated values in the reference [10], it

is valid that maximum A/D has 1.0 in the mooring line's strength design analysis.
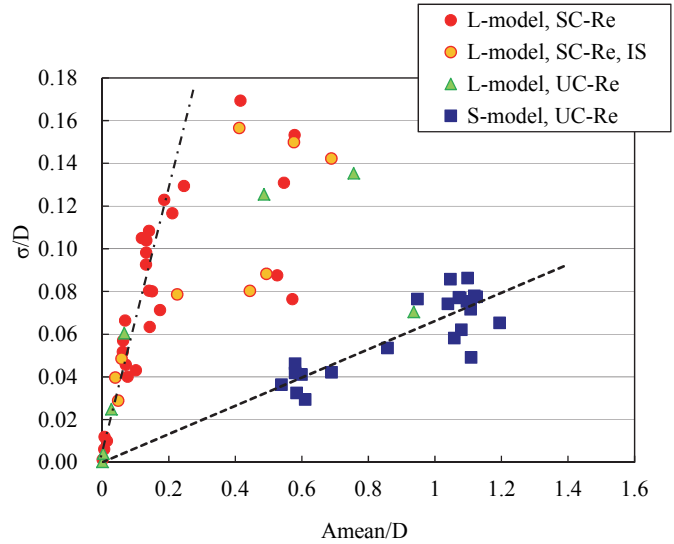

Figure 15. Standard diviation of mean amplitude of the models in transverse direction.

The data of additional model tests are included in the Figures 13 and 14 as 'S-model, Long'. Here, 'S-model, Long' data mean the results of a long length model rather than S-model (L/d =3.33), that were carried out in the same experimental system at the Actual sea model basin. The long S-model has Spar form with the averaged D =0.4m, L =2.2m (L/d =5.25) and W =233kg. The results of the long S-model are generaly same level against the ones of the original S-model. Then these figures suggest the results of the L-model would be able to use a indicator for many Spar type floaters, since the S-model results can be applied to wide L/d range Spar.

Figure 15 shows the standard diviation of mean amplitude of the models in transverse direction. As an indicator, two dotted lines are added for dominant results in the figure. The tendency of the experimental results of the L-model and the S-model is largely different. The standard diviations of mean amplitude of the L-model is larger than those of the S-model, that means the L-model condition which is SC-Re region results dominantly seems to be unstable.

To investigate detail this unstable situation, same condition experiments in V_r =8, 9 were repeatedly conducted. Figure 16 shows event probability of the L-model in V_r =8 and 9 with normal distribution and Table 2 represents the statistical parameters of the L-model shown in Figure 16. Normally about 25 extreme values that are blue dots in the Figure 12 are obtained from one test trial in 30s natural period stiffness, and half of them in 60s natural period stiffness in the 300m carriage running. 4~6 tests were carried out in the same condition in SC-Re region, and accumulate as one data.

The result of V_r=9 has wide distribution rather than that of V_r=8, and both cases distribution generally form to normal distribution. When growing up VIM amplitude in lock-in region, transverse motion is instable. The result of V_r=9 shows same level as the indicated values in the reference [10] shown in Figure 13 that maximum A/D has almost 0.4~0.6. In case of mooring line fatigue analysis, the distribution of A/D in VIM should be considered as shown in Figure 16.
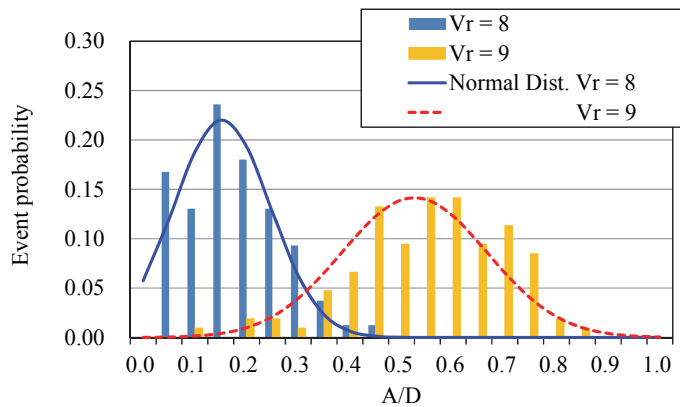

Figure 16. Event probability of transverse motion of the L-model in V_r=8 and 9 in SC-Re region tests with normal distribution.

Table 2. Statistical parameter of the L-model in V_r=8 and 9 shown in Figure 16.

Vr	8	9
Mean	0.152	0.525
Stand. Error	0.007	0.014
Median	0.139	0.534
Stand. Dev.	0.093	0.142
Variance	0.009	0.020
Kurtosis	-0.035	0.247
Skewness	0.533	-0.465
Range	0.439	0.734
Min	0.004	0.091
Max	0.443	0.825
Sample	161	106

Figure 17 shows the drag coefficient with VIM of the L-model. The marks and legends are same mean of the previous figures. The dotted line indecated in the reference [10] is much over values rather than the results of the L-model. On the other hands, the L-model results are same level of the full scale Spar measurement data that have 0.4~1.0 C_D in A/D=0.0~0.3[1]. The drag coefficient C_D is largely affected from the form of itself. In case of the strength and fatigue analysis, the way of setting the data without measured value in super critical

Reynolds number should be careful treatment, although the overestimated dotted line indicated in the figure as example leads to conservative result.
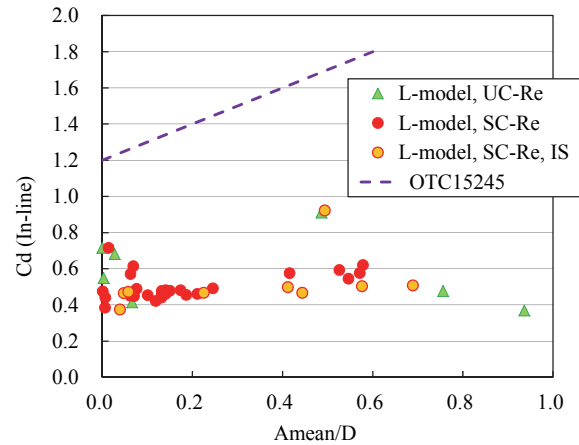

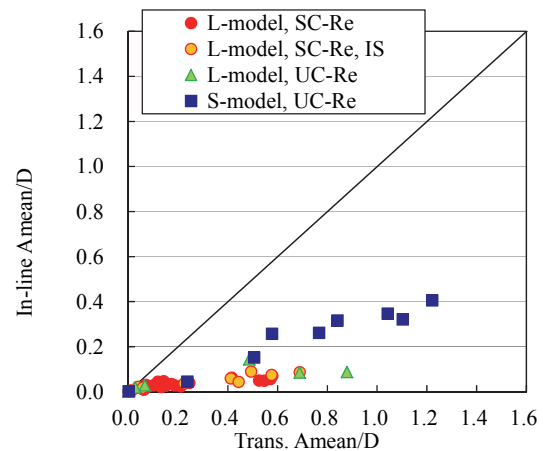**Figure 17.** Drag coefficient with VIM of the L-model.

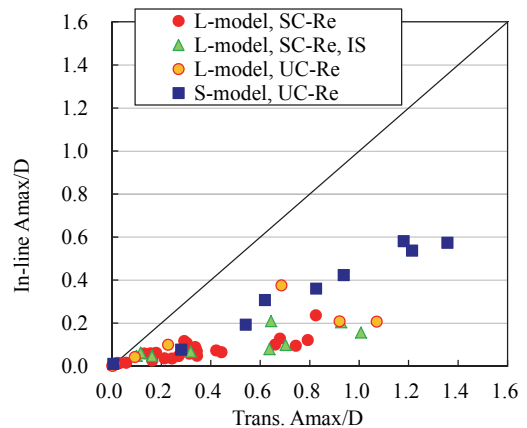**Figure 18.** Mean amplitude of the models in in-line motion comparing with that in transverse one.

Figure 19. Maximum amplitude of the models in in-line motion comparing with that in transverse one.

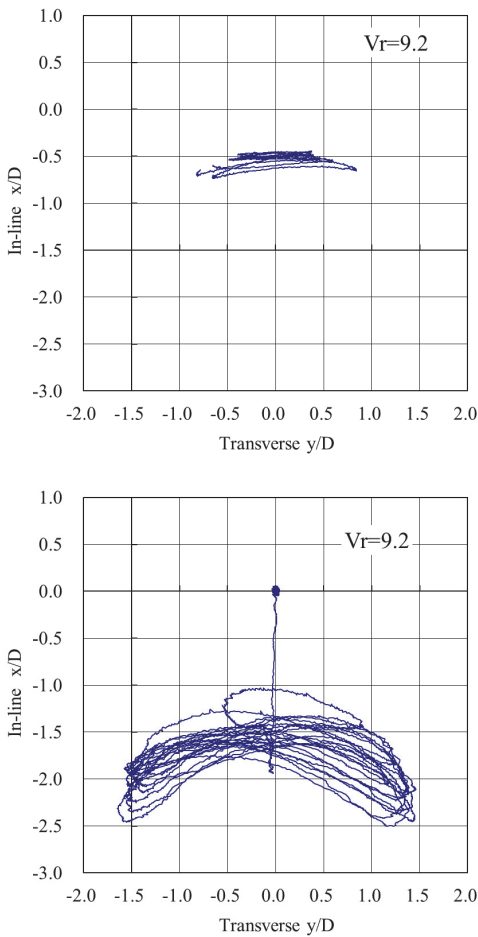6   Copyright © 2013 by ASME

Figure 20. Trajectories of the models in V_r =9.2 (upward; L-model, downward; S-model).

Figure 18 and Figure 19 show the mean and maximum amplitude of the models in in-line direction comparing with those in transverse direction, respectively. It seems that the in-line amplitude is set as 20% of transverse one on maximum amplitude in SC-Re region, and in case of mean value, 10% amplitude in same region. In the API Recommended Practice 2SK[4], it is indicated that "Field measurement data for a classic Spar with an equally spaced spread mooring system indicate inline A/D of 10% to 15% of the transverse A/D". In this case, it seems to be same amplitude level for the L-model. The S-model amplitude has trend to increase rather than that of the L-model.

In reference to Figure 18 and 19, trajectory of the models of the L-model and S-model in one test on V_r =9.2 shows in Figure 20 as an example. Each axis shows non-dimensional value devided by diameter D. Trajectory of the S-model has disarrayed trend rather than that of the L-model as plotted in Figure 18 and 19. In observation of water flow behind the model in towing, the L-model takes small and many voltexes in the water, however, in case of the S-model ralatively larger

voltexes come off from sarface of the circler cylinder, that means obviously the flow patterns of two models are different. Until getting enough accuracy level computational simulation result, it is important and necessary to do the experiment using a large model under super critical Reynolds number region.

CONCLUTIONS

VIM phenomenon using a large and small Spar models is investigated in the large towing tank and the experimental basin. As unique and precious trial, the tests in super critical Reynolds number region were conducted.

The results of this paper are summarized as follows:

1) VIM phenomenon completely differs bordering on critical Reynolds number. To assess accuracy level of VIM on full scale Spar structure, it is necessary to do the experiment in SC-Re region, that is in the super critical Reynolds number.
2) Maximum VIM amplitude of a simple Spar form is about 1.0 as the ratio of structure diameter, and maximum mean amplitude is about 0.6~0.7 in SC-Re region.
3) In-line amplitude is 20% level of transverse amplitude in the same Reynolds region.
4) VIM amplitude in SC-Re region varies in V_r = 9 level as near normal distribution. To assess exactly in the stage of mooring line fatigue analysis, it is better to use this knowledge and the result.
5) The drag coefficient of the Spar in VIM in SC-Re region is about 0.4~0.6.

ACKNOWLEDGMENTS

REFERENCES

[1] T-W. Yung, R. E. Sandström, S. T. Slocum, Z. J. Ding and R. T. Lokken, "Advancement of Spar VIV Prediction", The Offshore Technology Conference, OTC16343, 2004.
[2] Mehernosh Irani and Lyle Finn, "MODEL TESTING FOR VORTEX INDUCED MOTIONS OF SPAR PLATFORMS", OMAE2004-51315, 2004.

[3]   ISO, International Standard 19901-7, "Petroleum and natural gas industries -Specific requirements for offshore structures -, Part 7: Stationkeeping systems for floating offshore structures and mobile offshore units", 2012.

[4]   American Petroleum Institute, "API Recommended Practice 2SK – Design and Analysis of Stationkeeping Systems for Floating Structures", Third Edition, 2005.

[5]   Finnigan, T, Irani, M, and van Dijk, R, "Truss Spar VIM in Waves and Currents", OMAE 2005-67054, 2005.

[6]   Finnigan, T, and Roddier, D., "SPAR VIM MODEL TESTS AT SUPERCRITICAL REYNOLDS NUMBERS", OMAE2007-29160, 2007.

[7]   Roddier, D., Finnigan, T, and Liapis, S, "INFLUENCE OF THE REYNOLDS NUMBER ON SPAR VORTEX INDUCED MOTIONS (VIM): MULTIPLE SCALE MODEL TEST COMPARISONS", OMAE2009-79991, 2009.

[8]   Owen H. Oakley, Jr., Yiannis Constantinides, Claudia Navarro, Samuel Holmes, "MODELING VORTEX INDUCED MOTIONS OF SPARS IN UNIFORM AND STRATIFIED FLOWS", OMAE2005-67238, 2005.

[9]   Hoerner, S, F, "FLUID-DYNAMIC DRAG -Practical Information on AERODYNAMIC DRAG and HYDRODYNAMIC RESISTANCE-", 1965.

[10] Ken Huang, Xiaohong Chen, and Chi-Tat Kwan, "The Impact of Vortex-Induced Motions on Mooring System Design for Spar-based Installations", The Offshore Technology Conference, OTC 15245, 2003.